Mon. Not. R. Astron. Soc. **000**, 000–000 (0000) Printed 1 February 2008 (MN LATEX style file v2.2)

A search for 4750- and 4765-MHz OH masers in Southern Star Forming Regions

R.G. Dodson [1], S.P. Ellingsen [1]
[1] *School of Mathematics and Physics, University of Tasmania, GPO Box 252-21, Hobart, Tasmania 7001, Australia; Richard.Dodson@utas.edu.au, Simon.Ellingsen@utas.edu.au*

1 February 2008

ABSTRACT

We have used the Australia Telescope Compact Array (ATCA) to make a sensitive (5-$\sigma \simeq 100$ mJy) search for maser emission from the 4765-MHz $^2\Pi_{1/2}$ F=1→0 transition of OH. Fifty five star formation regions were searched and maser emission with a peak flux density in excess of 100 mJy was detected toward fourteen sites, with ten of these being new discoveries. In addition we observed the 4750-MHz $^2\Pi_{1/2}$ F=1→1 transition towards a sample of star formation regions known to contain 1720-MHz OH masers, detecting marginal maser emission from G348.550-0.979. If confirmed this would be only the second maser discovered from this transition.

The occurrence of 4765-MHz OH maser emission accompanying 1720-MHz OH masers in a small number of well studied star formation regions has lead to a general perception in the literature that the two transitions favour similar physical conditions. Our search has found that the presence of the excited-state 6035-MHz OH transition is a much better predictor of 4765-MHz OH maser emission from the same region than is 1720-MHz OH maser emission. Combining our results with those of previous high resolution observations of other OH transitions we have examined the published theoretical models of OH masers and find that none of them predict any conditions in which the 1665-, 6035- and 4765-MHz transitions are simultaneously inverted.

Key words: masers – stars:formation – ISM: molecules – radio lines : ISM

1 INTRODUCTION

High-mass star formation regions frequently exhibit OH maser emission, with thost most commonly observed being from the main-lines of the ground state $^2\Pi_{3/2}(J = 3/2)$ transitions, in particular the 1665-MHz ($F = 1 \rightarrow 1$) transition. Masing in the other ground state main-line transition at 1667 MHz ($F = 2 \rightarrow 2$) frequently accompanies the 1665-MHz masers, and in some sources the 1612- or 1720-MHz satellite-line transitions also exhibit maser action. Emission from the OH molecule has been detected towards star formation regions for all levels with energies less than approximately 500 K above the ground state. A number of searches towards star-forming regions have been undertaken for the higher exited OH transitions at 4765 MHz (Gardner & Martin-Pintado 1983; Cohen, Masheder & Walker 1991; Cohen, Masheder & Caswell 1995; Szymczak, Kus & Hrynek 2000) and 6035 MHz (Baudry et al. 1997; Smits 1994; Caswell & Vaile 1995) (the $^2\Pi_{1/2}$, F=1→0 and $^2\Pi_{5/2}$, F=3→3 transitions respectively).

For the $^2\Pi_{3/2}(J = 3/2)$ and $(J = 5/2)$ levels, the most commonly observed masing transitions towards star-forming regions are in each case one of the two main lines. However, for the $^2\Pi_{1/2}(J = 1/2)$ level, which is the lowest energy level of the $^2\Pi_{1/2}$ ladder, emission from the single main-line transition at 4750-MHz is very rare and the most commonly observed transition from this level is the F= 1 → 0 satellite line, analogous to the 1720-MHz transition in the ground-state. Masing emission from all of the transitions in the $^2\Pi_{1/2}$ ladder is rare and one obvious reason for this is that all the levels are at a higher energy than the two lowest levels in the $^2\Pi_{3/2}$ ladder level where masing emission is relatively strong and common. The reason for the 4765-MHz transition being the most common masing transition in the $^2\Pi_{1/2}$ ladder is that the $F = 1$ levels in $^2\Pi_{1/2}(J = 1/2)$ naturally become over populated with respect to the $F = 0$ due to selection rules (Elitzur 1977). 4765-MHz OH maser emission typically takes the form of a single narrow masing line and they are generally considered to be more highly variable

than ground-state transitions, the most spectacular example being Mon R2 (Smits, Cohen & Hutawarakorn 1998), which had a peak flux of 80 Jy in late 1997, but which we were unable to detect (5-σ = 80 mJy) in these observations. Intriguingly, Mon R2 is also unique in that it is the only 4765-MHz OH maser which has ever been found to exhibit any polarization (Smits, Cohen & Hutawarakorn 1998). Monitoring of a number of other 4765-MHz OH masers (Smits 1997; Szymczak, Kus & Hrynek 2000) shows that typically the degree of variability is much less than that for Mon R2. Analysis of the line width of the masers during variation by Szymczak et al. suggests that the masers are saturated, as do VLBI observations by Baudry et al. (1988).

Towards a small number of well studied OH maser sources (NGC7538, Sgr B2, W3(OH) & Mon R2) the 1720- and 4765-MHz OH maser transitions have been observed to be spatially coincident to within the relative positional errors of the observations (Palmer, Gardner & Whiteoak 1984; Gardner, Whiteoak & Palmer 1987; Baudry et al. 1988; Gray et al. 2001; Smits, Cohen & Hutawarakorn 1998). However, in most of these cases the positional errors are relatively large and the emission at the two frequencies is not necessarily coincident in velocity once Zeeman splitting is taken into account. The apparent association between 1720- and 4765-MHz OH masers was further strengthened by the results of the search of Cohen et al. (1995). They searched a sample of *IRAS* sources bright at 60 μm and found that all but one of the sites exhibitting 1720-MHz emission also showed 4765-MHz emission. MacLeod (1997) examined the relationship between 1720-, 4765- and 6035-MHz OH masers, again finding a strong correlation between the presence of 4765- and 1720- MHz OH masers. His analysis also shows that the vast majority of 4765-MHz maser sources exhibit 6035-MHz maser emission (there being only two exceptions).

While radiative pumps are generally favoured for excitation of the ground-state OH lines, it is possible to produce inversion in the 4765-MHz transition through either radiative or collisional processes (Elitzur 1977). Current theories prefer radiative excitation of all OH maser lines including those from the $^2\Pi_{1/2}$ ladder (Pavlakis & Kylafis 2000; Gray et al. 2001), although in the past collisional models have been put forward (Kylafis & Norman 1990). Much of the focus of previous modelling of 4765-MHz OH masers has been on finding conditions under which it is inverted at the same time as the 1720-MHz transition. Combining our observations of the $^2\Pi_{1/2}$, F=1$\rightarrow$1 and $^2\Pi_{1/2}$, F=1$\rightarrow$0 transitions with those of the ground-state and 6035-MHz transitions by Caswell (1997; 1998; 1999), (also observed at high-resolution with the ATCA), we have investigated the associations between the various OH transitions. These observations constitute a unique set of data, as for the first time a large number of sites have been observed in all the common OH maser transitions, at arcsecond resolution, with good sensitivity using the same instrument. Determining whether the different OH maser transitions are coincident is difficult as it requires full polarization VLBI observations to obtain the necessary spatial resolution and to account for the velocity shifts due to Zeeman splitting. From our observations and those of Caswell we are not able to determine coincidence of individual maser spots, however, they are able to show if the different transitions occur within the same maser cluster and whether the velocities are aligned.

It was suggested more than 30 years ago that since there are a number of OH maser transitions which are relatively common in star-formation regions, it should be possible to use observations of multiple transitions to test and constrain theoretical models of OH maser emission (Zuckerman & Palmer 1970). The only source which has been studied at high spatial resolution in a large number of OH transitions is W3(OH) (Reid et al. 1980; Baudry et al. 1988; Masheder et al. 1994; Baudry & Menten 1995; Baudry & Diamond 1998), for which Cesaroni & Walmsley (1991) produced a model which qualitatively matches the masers, thermal emission and absorption observed from the OH molecule towards the source. A similar approach has recently been used with some success for multiple methanol maser transitions towards sites of high-mass star formation (Cragg et al. 2001; Sutton et al. 2001) and the close relationship between OH and methanol masers (Caswell 1997) holds out the possibility of combining observations of both species to further constrain pumping models and the implied physical conditions (Cragg, Sobolev & Godfrey 2002). Observations such as these can be compared with the detailed studies of individual sources to determine to what degree the conditions inferred are generally applicable.

2 OBSERVATIONS AND DATA REDUCTION

The Australia Telescope Compact Array was used to make the observations of both the 4750- and 4765-MHz transitions, with rest frequencies 4750.656 MHz and 4765.562 respectively (Destombes et al. 1977). The configuration of six antennas yielded 15 baselines between 5 and 95 kλ for the 4765-MHz and between 1 and 90 kλ for the 4750-MHz observations. All pointings had 30 minutes or more of on-source observation, and the primary (and bandpass) calibrations were obtained from observations of PKS 1934-638. The correlator was configured with a 4-MHz bandwidth and 1024 spectral channels for each of the four polarisation products recorded. The sources were selected from those observed to exhibit either 6035- or 1720-MHz OH masers (Caswell 1997; Caswell 1999), or those previously reported to have 4765-MHz emission (Cohen, Masheder & Walker 1991; Cohen, Masheder & Caswell 1995; MacLeod 1997; Smits 1997). The observations spanned two epochs, 25-26 August 1999 for the 4750-MHz observations and 15-16 September 2000 for the 4765-MHz observations. Only those sites which showed 1720-MHz or 4765-MHz emission were searched for 4750-MHz emission. There are no reported southern sites of 4750-MHz emission other than that in Sgr B2 (Gardner, Whiteoak & Palmer 1987).

Data reduction was performed using the **miriad** and **karma** software packages and following the standard methods. With 1024 channels the effective velocity resolution at 4765-MHz is 0.3km s^{-1}. The 1-σ level over this bandwidth was $\approx$ 20 mJy per channel and the positional accuracy of the observations was typically 0.6$''$. We used a number of different methods to search for maser emission in our interferometric dataset. A vector averaged spectrum with a velocity resolution of 0.3 km s^{-1} was formed at the posi-

tions listed in tables 1 & 2. The velocity range covered by the spectrum and the measured 5-σ noise levels are listed in the same tables. In addition two image cubes were produced (both centred on the velocity listed in the tables), the first with an angular size of 256″ covering a velocity range of ±5 km s^{-1}with a 0.2 kms resolution and the second cube with an angular size of 150″ and a velocity range of ±20 km s^{-1} with a resolution of 1 km s^{-1}. The 1-σ noise levels in each of these images were approximately 30 and 12 mJy/beam respectively.

Unlike the ground-state OH transitions the $^2\Pi_{1/2}(J = 1/2)$ transitions are not expected to exhibit circular polarisation, as this level is diamagnetic (unlike all other OH rotational energy levels which are paramagnetic). None of the 4765-MHz masers observed have detectable levels of linear, or circular polarisation, the most stringent upper limits being 3.6% for linear polarisation and 5% for circular polarisation.

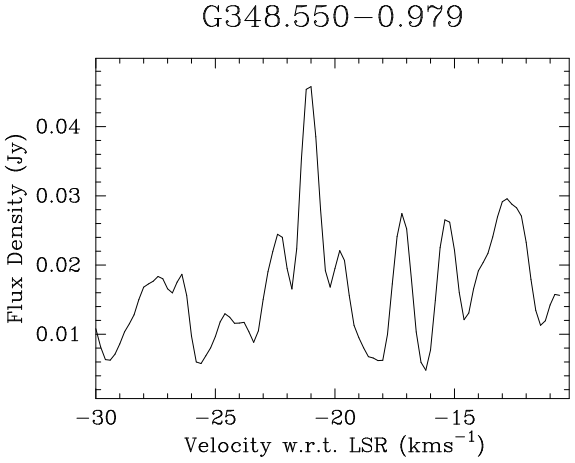

Figure 1. Spectrum of the marginal 4750-MHz OH maser detection towards G348.550-0.979

3 RESULTS

3.1 4750-MHz transition

A total of 17 star forming regions were searched for 4750-MHz OH emission, the position, velocity range and noise level for each site is given in Table 1. Only one of the 12 sites with 1720-MHz OH masers showed any sign of 4750-MHz emission, this being the marginal detection towards G348.550-0.979 (Fig. 1). The possible weak 4750-MHz OH maser emission at -21km s^{-1} does not match the velocity of the 1720- or 6035-MHz masers towards this site (Caswell 1999; Caswell & Vaile 1995), but does overlap that of the 1665- and 1667-MHz masers. The 4750-MHz transition has received very limited attention, with the only major searches being those by Gardner & Martin-Pintado (1983) and Cohen et al. (1991; 1995). The only site which has previously been reported to show 4750-MHz OH maser emission is S252 which was detected as an OH maser by Cohen et al. (1991) and which subsequent observations showed to be quite variable (Cohen, Masheder & Caswell 1995). One of the sources searched for 4750-MHz emission was Sgr B2, which was the first reported source to show emission from this transition (Gardner & Ribes 1971). Interferometric observations of the same source with a synthesised beamwidth of approximately 3″ show a similar spectrum (Gardner, Whiteoak & Palmer 1983). Our observations are at a higher spatial resolution and a combination of this and a relatively short integration time have produced a larger than average noise level for Sgr B2 which has meant that the 4750-MHz emission in this source is beneath our detection limit.

3.2 4765-MHz transition

A total of 55 star forming regions were searched for 4765-MHz OH emission, the position, velocity range and noise level for each site is given in Table 2. Fourteen likely 4765-MHz OH masers were detected towards nine different regions, two further sites showed signs of broader thermal emission, or possibly blended weak maser emission. These are listed in table 3 and spectra of each source are shown in figure 2. Ten of the sources have not previously been detected as 4765-MHz OH masers, the remaining previously reported in various papers, as indicated in the table. All of the new detections are relatively weak and below the sensitivity limit of most previous searches. We failed to detect emission in six sites where 4765 MHz emission had previously been reported (Mon R2, *IRAS*12073-6233, *IRAS*16183-4958, G338.925+0.557, *IRAS*17175-3544/NGC6334F, G10.623-0.383), a number of these exhibit thermal emission observed with single dishes. For *IRAS*16183-4958 and G10.623-0.383 the emission which has previously been reported is broad and most likely thermal in nature (Cohen, Masheder & Caswell 1995; Gardner & Martin-Pintado 1983). The thermal emission maybe resolved by our interferometric observations, and then our detection limits would then be considerably worse, as the sources would only contribute to the shorter baselines. For those sources where the emission is strong enough to plot intensity as a function of *uv* distance there is no sign of this. However, none of these are thermal sources. The most likely reason for the absence of emission from the other four sources, which have clearly been detected as masers in previous observations, is that the 4765-MHz maser is known to be highly variable, as reported for example by Smits et al. (1998).

A total of 38 sites of 6035-MHz OH masers were searched for 4765-MHz emission, resulting in ten detections (26%). In comparison, of the 12 1720-OH masers searched, 2 were observed to harbour 4765-MHz emission (17%) and both of these are also sites of 6035-MHz OH masers. This casts some doubt on the claimed predictive power of 1720/4765-MHz association, suggesting the presence of other excited OH transitions is at least as good a signpost for the presence of 4765-MHz OH masers, although with few detections the statistics are not compelling.

3.3 Comparison of different transitions

We have used our results to compare the emission we detect at 4765-MHz with published observations of other OH transitions toward the same site. This apparently simple task is complicated by the effect of Zeeman splitting on the

G240.316+0.071

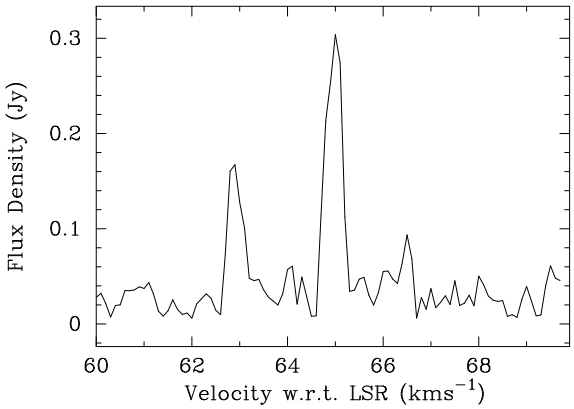

G294.511−1.621

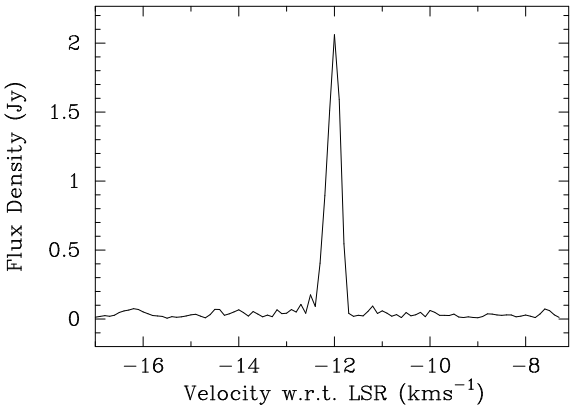

G309.921+0.479

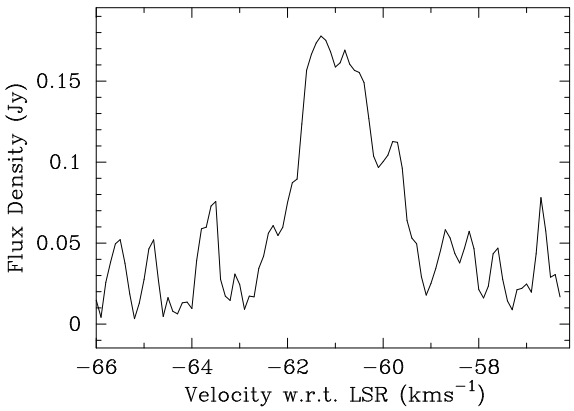

G328.304+0.436

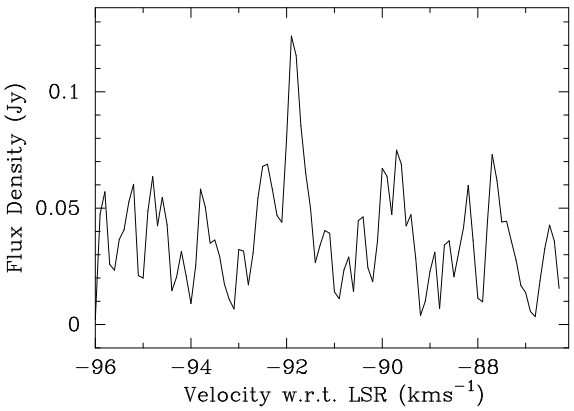

G328.307+0.430

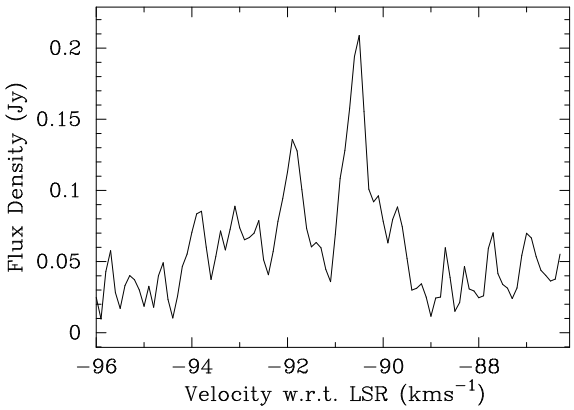

G328.808+0.633

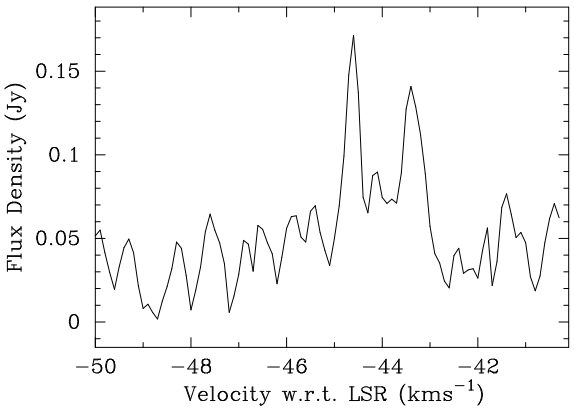

G333.135−0.431

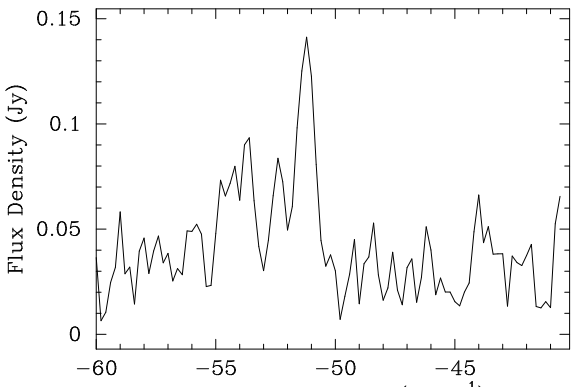

G333.135−0.431s

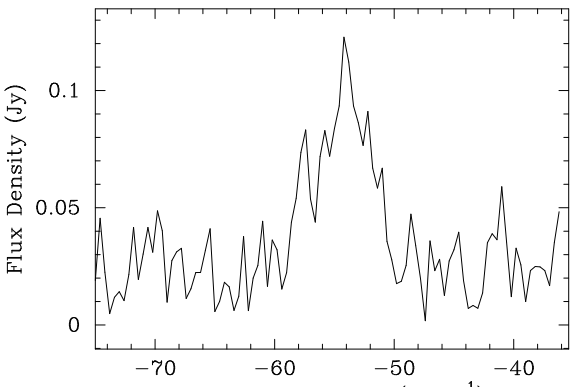

Table 1. Sources searched for 475O-MHz OH maser emission. The 5-σ limit column is for emission in a vector averaged spectrum at centred on the position, and covering the velocity range listed. References : a = Caswell (1997); b = Caswell (1999); c = Cohen et al. (1995); d = MacLeod (1997); e = Smits et al. (1998)

Source Name	Reference position Right Ascension (J2000)	Declination (J2000)	Velocity Range (km s^{-1})	5-σ Limit (Jy)	Central Velocity (km s^{-1})	References
Mon R2	06:07:47.832	-06:22:56.43	-40–60	0.2	-10.7	e
G294.511−1.621	11:35:32.208	-63:14:43.00	-60–40	0.1	-12,-12	a,b
*IRAS*12073−6233	12:10:00.360	-62:49:57.00	-20–80	0.4	32	c
G306.322−0.334	13:21:22.950	-63:00:28.40	-73–27	0.1	-23	b,d
G338.925+0.557	16:40:33.490	-45:41:37.00	-112– -12	0.1	-61.3	b,d
G339.622−0.121	16:46:06.030	-45:36:43.90	-87–12	0.1	-36.7	b,d
G340.785−0.096	16:50:14.838	-44:42:26.71	-146– -52	0.1	-105.6,-102	a,b
G345.003−0.224	17:05:11.205	-41:29:06.96	-75–24	0.1	-26.2,-29.3	a,b
G348.550−0.979	17:19:20.418	-39:03:51.65	-63–36	0.1	-13,-12.1	a,b
G351.417+0.645	17:20:53.370	-35:47:01.16	-60–39	0.2	-10,-10.4	a,b
*IRAS*17175−3544	17:20:54.945	-35:47:02.38	-60–39	0.2	-10	c
G351.775−0.536	17:26:42.559	-36:09:15.99	-50–49	0.1	-8.7,4	a,b
G353.410−0.360	17:30:26.189	-34:41:45.74	-70–29	0.2	-20.7,-19	a,b
G0.666−0.029	17:47:18.640	-28:22:54.60	22–120	0.5	72.6	a
G0.666−0.035	17:47:20.143	-28:23:06.18	22–120	0.5	67	a
G10.473+0.027	18:08:38.330	-19:51:47.90	10–109	0.2	64.7	b
G11.034+0.062	18:09:39.770	-19:21:23.60	-30–60	0.1	22.5	b

OH molecule, which shifts the observed velocity by differing amounts for the various transitions. Fortunately Caswell & Vaile (1995) have determined the magnetic field strength within the majority of the regions searched from observations of the 6035-MHz masers. We have used this information to calculate the velocity correction for each OH transition of interest. We have calculated the velocity shift due to Zeeman splitting for the various transitions using the method outlined in Elitzur (1992), and using the Lande-g factors as measured by Radford (1961). For the main-lines the Zeeman splitting is straight forward with the different σ-components all experiencing a velocity shift of essentially the same magnitude. For satellite lines the situation is more complex with potentially multiple Zeeman pairs being generated. From a theoretical standpoint, it isn't clear which pair will dominate as this may depend upon the pumping scheme, although observations tend to suggest that the pair with the largest Einstein A-coefficients dominate, at least for the 1720-MHz transition (Gray et al. 2001). Table 4 lists the amount by which RCP emission is shifted by the measured magnetic fields in each of the regions which show 4765-MHz OH masers. We have assumed that velocity shifts of 0.295, 0.177, 0.057 & 0.028 km s^{-1} mG^{-1} apply for the 1665-, 1667-, 1720- and 6035-MHz transitions respectively and that a positive B field will shift RCP emission to a more positive velocity (Caswell & Vaile 1995). The velocities in the table should therefore be subtracted from RCP velocities and added to LCP velocities to correct for Zeeman splitting. Where the alignment between different transitions is discussed for the individual sources below, the velocities have been corrected for the effects of Zeeman splitting (except where the observation is of total intensity).

We have used spectra in the literature to determine the strength of the other OH maser transitions at the velocity of the 4765-MHz OH maser emission. The results are listed in table 5 and demonstrate a number of general trends for the associations between the 4765-MHz emission and other common OH maser transitions. With one exception the 4765-MHz maser emission aligns in velocity with a peak in the 6035-MHz spectrum and since we know that the two transitions are spatially coincident to within 1 arcsecond then it seems likely that the emission from the two transitions is co-spatial. The 1665-MHz emission typically covers a wider velocity range than any of the other transitions and so it is not surprising that it overlaps the velocity range of the 4765-MHz emission. The 1665-MHz and 6035-MHz emission which aligns with the 4765-MHz are usually not the strongest peak in the spectrum. The 1665-MHz is often weaker than the 6035-MHz emission at the same velocity, and 1667-MHz emission is usually weak or in some cases entirely absent from the site. Caswell (1996) found 81% of main line OH maser sources have associated 6.7-GHz methanol emission. We find for our sample of fourteen 4765-MHz OH masers only 61% have associated methanol masers. This may indicate a tendency for the 4765-MHz masers to be more common towards regions without 6.7-GHz methanol masers, although the sample size is too small to reach definitive conclusions.

4 NOTES ON INDIVIDUAL SOURCES

4.1 Detections

G240.316+0.071

OH maser emission at this location was first detected in the 1665-MHz transition by MacLeod (1991). Subsequent observations by Caswell (1998) detected weak 1667-MHz emission at the same location, but offset in velocity from the 1665-MHz peak (Caswell, pers. comm.). The newly detected 4765-MHz maser has two spectral features at velocities of 63.0 and 65.2 km s^{-1}, neither of which match that of the strongest 6035-MHz emission at 63.6 km s^{-1} (Caswell & Vaile 1995). The secondary peak of the 6035-MHz emission matches the

Table 2. Sources searched for 4765-MHz OH maser emission. The 5-σ limit column is for emission in a vector averaged spectrum at centred on the position, and covering the velocity range listed. References : a = Caswell (1997) ; b = Caswell (1998) ; c = Caswell (1999) ; d = Cohen et al. (1995) ; e = Gardner & Martin-Pintado (1983); f = Smits et al. (1998).

Source Name	Reference position Right Ascension (J2000)	Declination (J2000)	Velocity Range (km s^{-1})	5-σ Limit (Jy)	Central Velocity (km s^{-1})	References
Mon R2	06:07:47.832	-06:22:56.43	-78–163	0.08	-10.7	f
G240.316+0.071	07:44:51.971	-24:07:42.32	-90–150	0.08	63.6	a
G284.351−0.418	10:24:10.680	-57:52:34.01	-103–138	0.11	4.7	a
G285.263−0.050	10:31:29.884	-58:02:18.48	-103–138	0.09	9.3	a
G294.511−1.621	11:35:32.208	-63:14:43.00	-105–135	0.09	-12,-12	a,c
*IRAS*12073-6233	12:10:00.360	-62:49:57.00	-106–135	0.09	32.0	d
G300.969+1.148	12:34:53.272	-61:39:39.91	-106–134	0.09	-37.8	a
G305.200+0.019	13:11:16.881	-62:45:54.72	-107–134	0.09	-33.2	a
G306.322−0.334	13:21:22.950	-63:00:28.40	-107–133	0.09	-23.0	c
G309.921+0.479	13:50:41.773	-61:35:10.08	-107–133	0.08	-59.8	a
G311.596−0.398	14:06:18.353	-62:00:15.29	-108–133	0.10	31.4	a
G311.643−0.380	14:06:38.742	-61:58:23.15	-108–132	0.09	33.8	a
G323.459−0.079	15:29:19.332	-56:31:21.26	-108–132	0.09	-70.2	a
G328.307+00.43	15:54:06.437	-53:11:41.11	-108–132	0.11	-90.4	a
G328.808+0.633	15:55:48.387	-52:43:06.69	-108–132	0.10	-45.7,-45,-43.5	a,a,c
G331.511−0.102	16:12:09.756	-51:28:37.84	-108–132	0.11	-90.0	a
G331.512−0.103	16:12:09.926	-51:28:37.06	-108–132	0.12	-86.8	a
G331.512−0.066	16:12:09.014	-51:25:47.69	-108–132	0.11	-86.0	a
G333.135−0.431	16:21:02.821	-50:35:12.01	-108–132	0.12	-50,-51.4	a,a
*IRAS*16183−4958	16:22:09.003	-50:05:59.66	-94–117	0.12	-50.0	d
G333.608−0.215	16:22:11.043	-50:05:56.52	-94–117	0.14	-51.6	a
G338.280+0.542	16:38:09.075	-46:11:03.10	-107–133	0.10	-56.8	a
G337.613−0.060	16:38:09.543	-47:04:59.89	-108–133	0.08	-42.0	a
G337.705−0.053	16:38:29.674	-47:00:35.85	-108–133	0.09	-50.6	a
G338.925+0.557	16:40:33.490	-45:41:37.00	-107–133	0.07	-61.3	c
G339.622−0.121	16:46:06.030	-45:36:43.90	-107–133	0.07	-36.7	c
G340.785−0.096	16:50:14.838	-44:42:26.71	-107–133	0.08	-105.6,-102	a,c
G345.010+1.792	16:56:47.580	-41:14:25.73	-107–134	0.09	-21.5	a
G343.929+0.125	17:00:10.907	-42:07:19.35	-107–133	0.08	13.6,11.9	a,b
G345.003−0.224	17:05:11.205	-41:29:06.96	-107–134	0.08	-26.2,-29.3	a,c
G345.698−0.090	17:06:50.599	-40:50:59.64	-106–133	0.08	-4.8	a
G347.628+0.149	17:11:50.888	-39:09:29.00	-106–134	0.08	-96.7	a
G348.550−0.979	17:19:20.418	-39:03:51.65	-106–134	0.08	-13.0,-12.1	a,c
G351.417+0.645	17:20:53.370	-35:47:01.16	-106–135	0.09	-10.0,-10.4	a,c
*IRAS*17175−3544	17:20:54.945	-35:47:02.38	-106–135	0.09	-10.0	d
G351.581−0.353	17:25:25.085	-36:12:46.08	-106–135	0.07	-93.8	a
G351.775−0.536	17:26:42.559	-36:09:15.99	-106–135	0.09	-8.7,4	a,c
G353.410−0.360	17:30:26.189	-34:41:45.74	-105–134	0.08	-20.7,-19	a,c
G354.724+0.300	17:31:15.547	-33:14:05.59	-105–135	0.08	90.2	a
G355.344+0.147	17:33:29.055	-32:47:58.77	-104–135	0.08	18.0	a
G359.138+0.031	17:43:25.638	-29:39:18.29	-104–136	0.10	-1.8	a
G0.666−0.029	17:47:18.640	-28:22:54.60	-106–139	0.18	72.6	a
G0.666−0.035	17:47:20.143	-28:23:06.18	-106–139	0.18	67.0	a
G10.473+0.027	18:08:38.330	-19:51:47.90	-100–140	0.09	64.7	c
G11.034+0.062	18:09:39.770	-19:21:23.60	-100–140	0.08	22.5	c
G11.904−0.141	18:12:11.437	-18:41:29.05	-100–140	0.09	42.8	a
G10.623−0.383	18:10:28.610	-19:55:49.10	-100–140	0.09	-2.0,-1.5	b,e
G15.034−0.677	18:20:24.811	-16:11:34.14	-100–140	0.17	21.2	a
W49N	19:10:12.006	+09:06:11.25	-90–150	0.11	2.0	d

weaker 4765-MHz feature at 62.8 km s^{-1}. There is no 6.7-GHz methanol maser emission towards this site.

G240.311+0.074

This newly detected maser source is offset to the south by approximately 20″ from G240.316+0.071. High resolution observations by Caswell at 1665- and 6035-MHz (1997; 1998) have not reported any emission towards this location. A search of SIMBAD reveals no other astrophysical objects within 10″ of this site.

Table 3. Sources with detected 4765-MHz OH emission. References : *=new source, a=Cohen, Masheder & Caswell (1995); b=Gardner & Ribes (1971); c=Smits (1997); d=Zuckerman & Palmer (1970).

Source Name	4765-MHz Maser Right Ascension (J2000)	Declination (J2000)	Peak Flux Density (Jy)	Velocity of Peak (km s^{-1})	Width of Peak (km s^{-1})	References
G240.316+0.071	07:44:51.982±0.004	-24:07:42±3	0.31,0.17	65.0,62.9	0.4,0.4	*
G240.311+0.074	07:44:52.00±0.01	-24:07:22±9	0.11	66.7	0.4	*
G294.511−1.621	11:35:32.232±0.003	-63:14:43.12±0.02	2.02	-12.0	0.3	c
G309.921+0.479	13:50:41.77±0.03	-61:35:09.9±0.2	0.17	-60.9	2.1	*
G328.304+0.436	15:54:03.94±0.06	-53:11:32.2±0.2	0.12	-91.8	0.4	*
G328.307+0.430	15:54:06.38±0.03	-53:11:41.0±0.1	0.16	-90.5	0.9	*
G328.808+0.633	15:55:48.33±0.04	-52:43:06.5±0.2	0.17	-44.6	0.3	*
G328.809+0.633	15:55:48.42±0.05	-52:43:06.2±0.2	0.14	-43.4	0.5	*
G333.135−0.431	16:21:02.80±0.05	-50:35:10.1±0.2	0.14	-51.2	0.8	*
G333.135−0.431s	16:21:02.78±0.04	-50:35:12.7±0.2	0.10	-54.3	5.9	*,Thermal
G353.410−0.360	17:30:26.182±0.001	-34:41:46.15±0.03	1.78	-20.8	0.4	a,c
Sgr B2/G0.666−0.035	17:47:20.143	-28:23:06.18	0.07	49.6	6.5	b, Thermal
G11.904−0.141	18:12:11.437±0.002	-18:41:29.0±0.1	1.0	41.8	0.4	*
W49SW	19:10:10.9±0.3	+09:05:23±5	0.24,0.12	8.6,11.9	0.4,0.2	a,c
W49N	19:10:13.51±0.01	+09:06:15±2	0.63	2.3	0.6	d,c
W49NW	19:10:14.3±0.2	+09:06:24±3	0.34	2.7	0.6	*

Table 4. Velocity corrections for the effect of Zeeman splitting for RCP emission in the 1665-, 1667-, 1720- and 6035-MHz OH transitions. The magnetic field estimates listed are taken from Caswell & Vaile (1995), except for W49N & W49NW which are from Gaume & Mutel (1987).

Source Name	Magnetic Field (mG)	4765-MHz Velocity (km s^{-1})	Velocity correction for OH transition (for RCP) 1665-MHz (km s^{-1})	1667-MHz (km s^{-1})	1720-MHz (km s^{-1})	6035-MHz (km s^{-1})
G240.316+0.071	< 0.5	+62.9,65.0	<0.15	<0.09	<0.03	< 0.01
G294.511−1.621	+1.1	-12.0	0.32	0.19	0.06	0.03
G309.921+0.479	-2.5 – +3.5	-60.9	-0.74–1.03	-0.44–0.62	-0.14–0.20	-0.07–0.10
G328.307+0.430	3.2	-90.5	0.94	0.57	0.18	0.09
G328.808+0.633	-4.3	-44.6	-1.27	-0.76	-0.24	-0.12
G328.809+0.633	-4.3	-43.4	-1.27	-0.76	-0.24	-0.12
G333.135−0.431	-3.3	-51.2	-0.97	-0.58	-0.19	-0.09
G353.410−0.360	-1.1	-20.8	-0.32	-0.19	-0.06	-0.03
G11.904−0.141	< 0.5	+41.8	<0.15	<0.09	<0.03	< 0.01
W49SW	-4.3	+8.6,11.9	-1.27	-0.76	-0.24	-0.12
W49N	3.1–7.5	+2.3	0.91–2.21	0.55–1.32	0.18–0.42	0.09–0.21
W49NW	3.1–7.5	+2.7	0.91–2.21	0.55–1.32	0.18–0.42	0.09–0.21

G294.511-1.621

The ground-state OH maser emission at this location was detected by Braz et al. (1989) towards an H_2O maser source. The 4765-MHz OH maser emission was discovered by Smits (1997) and is the strongest detected in this survey with a peak flux density of 2 Jy. The velocity and position of the 4765-MHz emission matches that of the 6035-MHz emission at -12 km s^{-1} (Caswell & Vaile 1995). A minor peak of the 1665-MHz aligns with the 4765-MHz maser and there is probably 1667-MHz emission at the same velocity, but the ATCA observation is of total intensity and so cannot be corrected for Zeeman splitting (Caswell, pers. comm.).

G309.921+0.479

The 4765-MHz OH emission in this source is relatively broad (2.1 km s^{-1}) and may be quasi-thermal emission or a blend of a number of weak maser features. The secondary peak (-59.8 km s^{-1}) matches the peak of the 6035-MHz maser, the broad emission is echoed in the weaker broad emission in the 6035-MHz spectrum (Caswell & Vaile 1995). The magnetic field in this region is confused and so determining the alignment for the 1665- and 1667-MHz transitions is less certain, it appears that in both cases the 4765-MHz emission aligns with lesser peaks (Caswell & Haynes 1987).

G328.304+0.436

This newly detected maser source is offset to the south-west by approximately 24″ from G328.307+0.430. As for G240.311+0.074, Caswell does not report any emission at 1665- or 6035-MHz (1997; 1998) towards this location, and a SIMBAD search finds nothing within 10″.

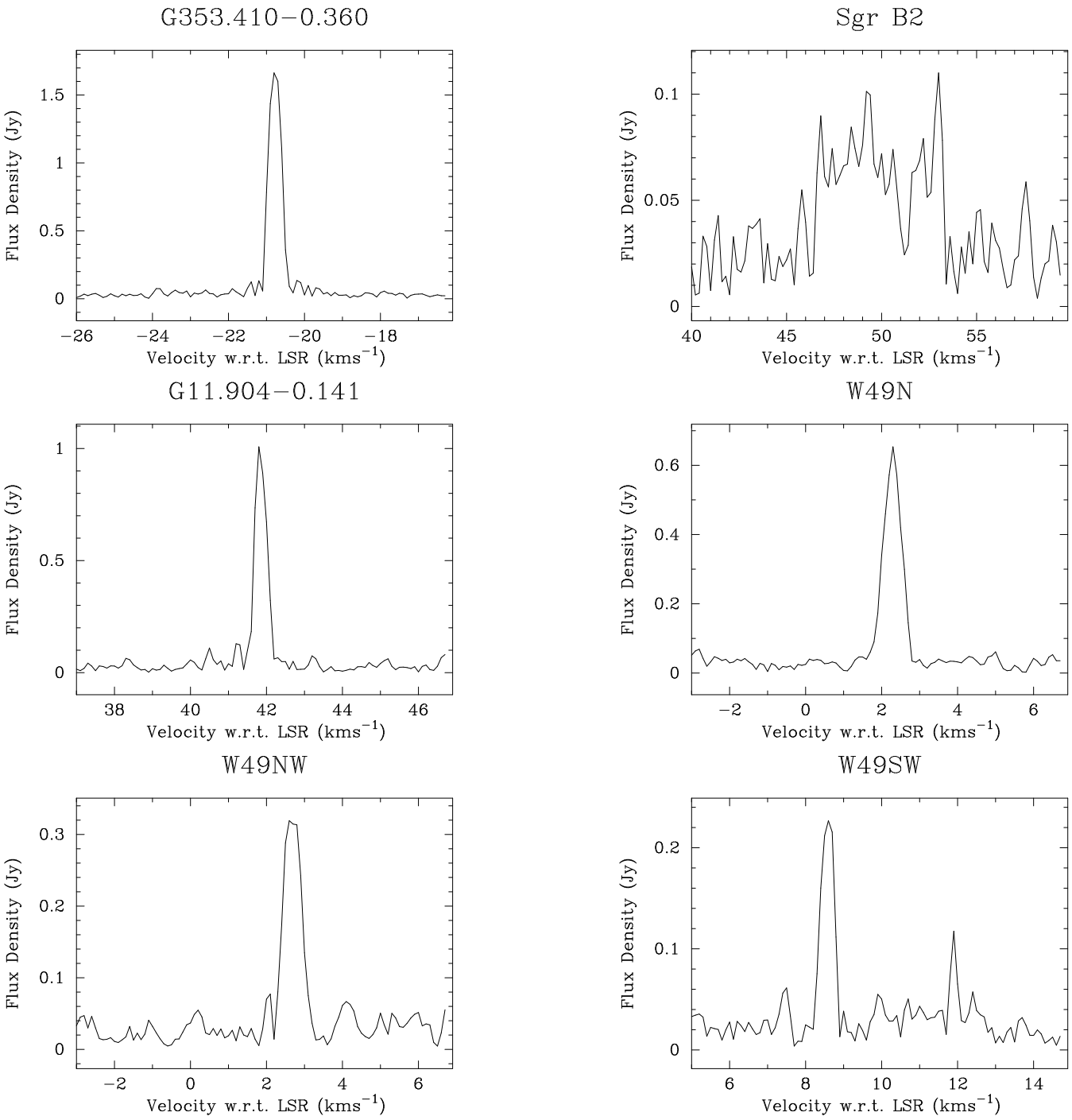

Figure 2 – *continued*

G328.307+0.430

This new 4765-MHz detection has two features at -90.5 and -92.0 km s^{-1}, it was not detected in previous surveys, the most sensitive of which was Cohen et al. (1995). The 1667-MHz emission towards this source is weak and unlike the majority of the other regions there is no 6.7-GHz methanol maser emission at this site. The stronger 4765-MHz emission matches the velocity of a 10 Jy LCP peak at 1665-MHz, although there is no Zeeman pair (Caswell, Haynes & Goss 1980). The 6035-MHz emission is also aligned in velocity with the strongest 4765-MHz maser.

G328.808+0.633/G328.809+0.633

Caswell (1997) reports two nearby sources each of which exhibit both 6035 MHz OH and 6.7-GHz methanol masers. To within the accuracy of our resolution we find 4765-MHz OH maser emission to also be present at both sites. G328.809+0.633 is offset from the HII region and also ex-

Table 5. The flux density of 1665-, 1667-, 1720- and 6035-MHz OH transitions at the velocity of the 4765-MHz transition (after accounting for the shift due to Zeeman splitting). The reported flux densities are for RCP emission, except where (L)=LCP or (I)=Total intensity is indicated. Where no information is available for a particular transition than column has been left blank. References : a = Braz et al. (1989); b = Caswell (pers. comm.); c = Caswell (1998); d = Caswell (1999); e = Caswell & Haynes (1983a); f = Caswell & Haynes (1983b); g = Caswell & Haynes (1987); h = Caswell & Vaile (1995); i = Caswell, Haynes & Goss (1980); j = Gaume & Mutel (1987); k = Haynes & Caswell (1977); l = MacLeod (1991)

Source Name	4765-MHz Velocity (km s^{-1})	Flux Density at 4765-MHz Velocity 1665-MHz (Jy	1667-MHz (Jy)	1720-MHz (Jy)	6035-MHz (Jy)	References
G240.316+0.071	+62.9	1.8	<0.05	<0.5	0.2	c,b,h,l
G240.316+0.071	+65.0	<0.05	<0.05	<0.5	<0.1	c,b,h,l
G294.511−1.621	-12.0	2.0	0.6(I)		4.6	a,b,c,h
G309.921+0.479	-60.9	1.0	1.0	<1.0	2.0	g,h
G328.307+0.430	-90.5	10.0(L)	<0.5	<1.2	1.4	h,i,k
G328.808+0.633	-44.6	11.0(L)	12.0(L)	<0.5	1.5	d,h,i
G328.809+0.633	-43.4	6.0	1.5	<0.5	5.0	b,d,h,i
G333.135−0.431	-51.2	6.0	2.0	<1.2	2.0	i,h,k
G353.410−0.360	-20.8	<0.5	<0.5	<0.5	17.5	e,h,j
G11.904−0.141	+41.8	0.5(L)	0.5		0.6	f,h

hibits 1720-MHz OH emission. The velocity of the 1720-MHz OH maser in the total intensity observation of Caswell (1999) is offset by +0.2 km s^{-1} from the 4765-MHz peak. Full polarization observations reveal that after correction for Zeeman splitting the 1720-MHz emission does not align with the 4765-MHz maser peak (Caswell pers. comm.). There appears to be peaks in the 6035-MHz spectrum which correspond to the two 4765-MHz peaks (Caswell & Vaile 1995) and the strongest 1665-/1667-MHz emission covers the same velocity range (Caswell, Haynes & Goss 1980).

G333.135-0.431/G333.135-0.431s

There are two sites of 6035-MHz OH maser emission in this region. G333.135-0.431 contains the stronger emission and doesn't have an associated 6.7-GHz methanol maser, while G333.135-0.431s contains weaker 6035-MHz emission covering a larger velocity range and with weak 6.7-GHz methanol masers (Caswell 1997). The strong narrow 4765-MHz maser lies towards the first of these sites and matches the velocity of secondary peaks in all of the 1665-, 1667 and 6035-MHz transitions (Caswell, Haynes & Goss 1980; Caswell & Vaile 1995). The 4765-MHz emission towards G333.135-0.431s appears to be thermal and matches the velocity of the strongest 1665-/1667-MHz absorption, broad weaker 6035-MHz emission and broad weak 6.7 GHz methanol emission (Caswell, Haynes & Goss 1980; Caswell 1997).

G353.410-0.360

This was the strongest source detected by Cohen et al.(1995), and has not varied more than 6%. The 4765-MHz peak matches the velocity and position of the peak of the complex 6035-MHz spectrum, but it isn't clear whether or not the 1720-MHz emission matches the 4765-MHz velocity. The observations of Gaume & Mutel (1987) have coarse spectral resolution, while the total intensity observations of Caswell (1999) show a significant velocity offset, suggesting that the transitions probably do not align. The 1665- and 1667-MHz velocity ranges do not overlap with the 4765-MHz emission (Caswell & Haynes 1983a).

Sgr B2/G0.666-0.035

4765-MHz maser emission was first observed towards Sgr B2 by Gardner & Ribes (1971) at 60.8 and 61.4 km s^{-1} using the Parkes telescope. It was not seen by Effelsburg or VLA observations in 1983 and 1984 (Gardner & Martin-Pintado 1983; Gardner, Whiteoak & Palmer 1987). We find no narrow emission, but a weak and broad feature at a lower velocity which matches the broad-band observations of Gardner & Ribes (1971). This does not match the velocity of the 6035-MHz or 1720-MHz maser emission (Caswell & Vaile 1995; Gaume & Mutel 1987).

G11.904-0.141

The 4765-MHz maser emission from this new detection peaks at 41.8 km s^{-1} and aligns in velocity with the weaker of the two 6035-MHz maser peaks (Caswell & Vaile 1995). It also matches the velocity of the strongest LCP features in the 1665- and 1667-MHz spectra (Caswell & Haynes 1983b; Forster & Caswell 1989).

W49N and W49SW

Previous single dish observations have not been able to discriminate between the 4765-MHz OH emission at 2.2 km s^{-1} from the northern portion of this region with the emission at 8.2 km s^{-1} from the south west portion, 1.2′ away. Two features can be found in W49N, the stronger peaking at 2.1 km s^{-1}, the other peaking at 2.6 km s^{-1}. The two sources are offset by 12″ to the East. Smits (1997) has summarised the previous observations of the 4765-MHz OH maser emission in this source, and we detect all the spectral features observed by him and confirm a velocity of 8.6 km s^{-1} for the emission towards W49SW. We also detect a previously unreported maser towards the same region

at a velocity of 11.9 km s^{-1}. No feature was observed corresponding to the report of Smits (1997) of a weak broad emission around 3.6 km s^{-1}, but the intensity of all the observed features appears to have declined in the intervening period. The OH maser emission in this region is very complex and we have not attempted to determine the alignment of the 4765-MHz emission with other transitions as the potential for confusion is too great. This is exacerbated by the fact that for these northern sources our positional errors in declination are several arcseconds. However, the position Caswell & Vaile (1995) report for the strongest 6035-MHz emission matches the 4765-MHz maser W49SW.

4.2 Non detections

Mon R2

Mon R2 is one of the best studied 4765-MHz masers and is known to be highly variable and also show polarized emission (Smits, Cohen & Hutawarakorn 1998). Emission from the 4765-MHz transition towards this source was first reported by Gardner & Martin-Pintado (1983). Cohen et al. (1991) failed to detect any emission, but it was later detected by Cohen et al. (1995). Smits et al. monitored it closely from late 1994 through to mid-1997 and it reached a peak flux density of 80 Jy in 1997, at times doubling in intensity every 19 days (Smits, Cohen & Hutawarakorn 1998). When observed by Szymczak et al. (2000) in 1998 it had declined by an order of magnitude from its peak, to a flux density 6 Jy and it subsequently declined further to below the detection limits for the Hartebeesthoek radio telescope (Smits, pers. comm.). We also find no emission in this survey with an upper limit of 80 mJy, 3 orders of magnitude lower than its strongest recorded flux density.

IRAS*12073-6233*

This source was discovered by Cohen et al. (1995) and subsequently monitoring by Smits (1997) observed it to reach a maximum flux density of 1.2 Jy in 1994.8, which afterwards fell at about 0.5 Jy per year. Our non-detection of this source is consistent with this decline continuing.

IRAS*16183-4958*

This weak detection in the survey of Cohen et al. (1995), was not detected in our observations. Had it remained constant it would have been well above our detection limit and so must have decreased in intensity by at least 50% in the intervening period.

G338.925+0.557

This source was detected in a search of 1720-MHz OH maser sources by MacLeod (1997). MacLeod reports a peak flux density of 1.5 Jy, while we fail to detect any emission stronger than 70 mJy, indicating that this source decreased in intensity by more than a factor of 20 in the four year period between the two sets of observations.

IRAS*17175-3544/NGC6334F*

This weak detection in the survey of Cohen et al. (1995), was not detected in our observations. If it had remained constant it would have been well above our detection limit and so must have decreased in intensity by at least 67% in the intervening period.

5 DISCUSSION

The association between 1720- and 4765-MHz OH masers has only been studied in detail towards W3(OH). Of the two 4765-MHz masers we detected which may be closely associated with 1720-MHz OH emission, for one the velocity (after correction for Zeeman splitting) doesn't match and for the other it may align, but further investigation is required. VLBI observations of the 1720-MHz OH masers by Masheder et al. (1994) found that although the two transitions came from the same spatial location (within the relative uncertainties), the velocities did not align. Intriguingly, more recent MERLIN observations by Gray et al. (2001) found both spatial and velocity alignment between the two transitions. One possible explanation for this is that the 4765-MHz OH masers can be highly variable and it is not unknown for masers features to disappear and new features appear at nearby, but different velocities (e.g. W49N). This highlights the major pitfall in attempting to test theoretical models with multi-transition observations; variability over time and the effects of observations at different spatial and spectral resolutions all add uncertainty to comparisons of the different transitions. Our observations suggest that 4765-MHz OH masers are frequently not accompanied by 1720-MHz OH masers, but further high resolution, full polarization observations of the 1720-MHz OH masers in southern star forming regions are required to confirm this.

It is clear from literature that current theoretical OH maser models are complicated by unknown, or poorly known excitation rates for the pumping paths. The models of Gray et al. (1992) produce parameter ranges where both 1720- and 4765-MHz transitions are inverted with local temperatures of 125K, high densities and large velocity gradients. These are the only conditions under which 4765-MHz masers are significantly excited and the 6035-MHz line is strongly suppressed under these conditions. This is contrary to our observations in which 4765- and 6035-MHz masers are commonly present together.

In contrast the models of Pavlakis & Kylafis (1996b), which use different collision rates find 4765-MHz masers are only excited with *low* velocity gradients, while 1720-MHz emission is only exited with *high* velocity gradients. Pavlakis & Kylafis (1996b) find that the 4765-MHz masers only appear at higher densities than the ground state main lines and there is essentially no overlapping density range. This contrasts with our observations that the 4765-MHz OH masers are typically associated with the 1665-MHz transition. Modelling of the 6035-MHz OH masers is covered in a separate paper (Pavlakis & Kylafis 2000) and the issue of the association between 4765- and 6035-MHz masers is not covered. Through comparison of the plots from the two papers we can deduce that the two transitions are both inverted for the narrow molecular hydrogen density range of $4 \times 10^6 - 10^7 \mathrm{cm}^{-3}$,

with 150 K gas, 200 K dust temperatures and large optical depth (Pavlakis & Kylafis 1996b - Fig. 6d ; 2000 - Fig. 9d). Once again, for these physical conditions the ground state main lines are not inverted. Pavlakis & Kylafis have many more free parameters in their modelling, complicating interpretation. It is also possible that there are, unpublished parameter combinations that excite 4765-, with 1665-, 1720- and/or 6035-MHz.

Pavlakis and Kylafis (1996b) find a number of different parameter combinations which produce 1720-MHz OH masers, but the strongest emission occurs in the absence of far infrared emission, at high densities and large velocity gradients. Under these conditions they also predict that the 4750-MHz transition should produce bright masers. Our search failed to detect any strong 4750-MHz masers associated with 1720-MHz OH masers, which suggests that the one of the other parameter combinations must be responsible for the 1720-MHz OH masers.

6 CONCLUSIONS

We report the discovery of ten new $^2\Pi_{1/2}$ F=1→0 4765-MHz OH maser emission sites, more than doubling the number reported in the southern hemisphere. We have found that the frequently purported association between 1720-MHz OH masers and 4765-MHz emission is not as strong as the correspondence between 6035- and 4765-MHz masers. The 4765-MHz OH masers are relatively weak and uncommon compared to the 1665-, 1667- and 6035-MHz transitions and so, except for attempting to explain the 1720-/4765-MHz association, the models of Pavlakis & Kylafis (1996a; 1996b; 2000) and Gray et al. (1992; 2001) largely ignore this transition. Examination of published spectra of the 1665-, 1667-, 1720- and 6035-MHz OH transitions shows that after correcting for the effects of Zeeman splitting the 4765-MHz OH masers are characterised by a close association with the 6035-MHz transition, modest 1665-MHz emission and weak or absent 1667-MHz emission. None of the current models of OH maser emission produces results which are qualitatively consistent with these findings. We suggest that the best indicator of likely 4765-MHz OH masers is the presence of other excited state transitions, such as the 6035-MHz, but that these regions also frequently possess the correct physical conditions to produce satellite-line masers from the ground-state. Further theoretical modelling is required to determine ranges of physical parameters which can produce OH maser emission with the same characteristic as we observe. In addition, we failed to find any sites where 1720-MHz and 4750-MHz OH emission are produced simultaneously despite this being a well populated condition in theoretical models for certain parameter ranges.

Determining the relative intensity of emission from different OH transitions by comparison with published observations has several major sources of uncertainty, in particular temporal variability and instrumental effects. To overcome this it would be highly desirable to be able to make simultaneous, or quasi-simultaneous full polarization observations of a large number of OH transitions, at high spatial and spectral resolution. Such observations are possible, for example, with the ATCA. The 19 lowest frequency OH transitions fall within the frequency coverage and it is possible to observe many, or all of these within a single observing session. This type of observation would clearly provide much stronger observational constraints and tests for theoretical modelling than are currently available.

A number of the newly discovered 4765-MHz OH masers (G240.331+0.074 &G328.304+0.436) are not associated with previously detected sites of ground-state OH masers or other common sign-posts of star formation, such as *IRAS* sources. These masers are very weak, but further investigation is warranted to confirm their existence and to try and determine whether they are associated with high-mass star formation, or some other astrophysical phenomena.

7 ACKNOWLEDGMENTS

We would like to thank J.L. Caswell for providing unpublished Parkes and ATCA spectra for a number of sources and communication of unpublished results. The Australia Telescope Compact Array is part of the Australia Telescope, funded by the Commonwealth of Australia for operation as a National Facility, and managed by CSIRO. This research has made use of the SIMBAD database operated at CDS, Strasbourg, France. This research has made use of NASA's Astrophysics Data System Abstract Service.

REFERENCES

Baudry, A., Diamond, P. J. 1998, A&A 331, 697
Baudry, A., Diamond, P. J. 1991, A&A 247, 551
Baudry, A., Menten, K. M. 1995, A&A 298, 905
Baudry, A., Diamond, P. J., Booth, R. S., Graham, D., Walmsley, C. M. 1988, A&A 201, 105
Baudry, A., Desmurs, J. F., Wilson, T. L., Cohen, R. J. 1997, A&A 325, 255
Braz, M. A., Scalise Jr., E., Gregorio Hetem, J. C., Monterio de Vale, J. L., Gaylard, M. 1989, A&ASS 77, 465
Caswell, J. L. 1996, MNRAS 279, 79
Caswell, J. L. 1997, MNRAS 289, 203
Caswell, J. L. 1998, MNRAS 297, 215
Caswell, J. L. 1999, MNRAS 308, 683
Caswell , J. L., Haynes, R. F. 1983, Aust. J. Phys. 36, 361
Caswell , J. L., Haynes, R. F. 1983, Aust. J. Phys. 36, 417
Caswell , J. L., Haynes, R. F. 1987, Aust. J. Phys. 40, 215
Caswell, J. L., Vaile, R. A. 1995, MNRAS 273, 328
Caswell , J. L., Haynes, R. F., Goss, W. M. 1980, Aust. J. Phys. 33, 639
Caswell, J. L., Vaile, R. A., Forster, J. R. 1995, MNRAS 277, 210
Cesaroni, R., Walmsley, C. M. 1991, A&A 241, 537
Cohen, R. J., Masheder, M. R. W., Walker, R. N. F. 1991, MNRAS 250, 611
Cohen, R. J., Masheder, M. R. W., Caswell, J. L. 1995, MNRAS 274, 808
Cragg, D. M., Sobolev, A. J., Ellingsen, S. P., Caswell, J. L., Godfrey, P. D., Salii, S. V., Dodson, R. G. 2001, MNRAS 323, 939
Cragg, D. M., Sobolev, A. J., Godfrey, P. D. 2002, MNRAS in press.
Desmurs, J. F., Baudry, A., Wilson, T. L., Cohen, R. J., Tofani, G. 1998, A&A 334, 1085
Destombes, J. L., Marliere, C., Baudry, A., Brillet, J. 1977, A&A 60, 55
Elitzur, M. 1977, MNRAS 179, 143
Elitzur, M. 1992, Astronomical Masers, Kluwer, Dordrecht
Forster, J. R., Caswell, J. L. 1989, A&A, 213, 339

Gardner, F. F., Martin-Pintado, J. 1983, A&A, 121 265
Gardner, F. F., Ribes, J. C. 1971, Astrophysical Letters 9, 175
Gardner, F. F., Whiteoak, J. B., Palmer, P. 1983, MNRAS 205, 297
Gardner, F. F., Whiteoak, J. B., Palmer, P. 1987, MNRAS 225, 469
Gaume, R. A., Mutel, R. L. 1987, ApJSS 65, 193
Gray, M. D., Field, D., Doel, R. C. 1992, MNRAS 262, 555
Gray, M. D., Cohen, R. J., Richards, A. M. S., Yates, J. A., Field, D. 2001, MNRAS 324, 643
Haynes, R. F., Caswell , J. L. 1977, MNRAS 178, 219
Kylafis, N. D., Norman, C. 1990, ApJ 350, 209
MacLeod, G. C. 1991, MNRAS 252, 36p
MacLeod, G. C. 1997, MNRAS 285, 635
Masheder, M. R. W., Field, D., Gray, M. D., Migenes, V., Cohen, R. J., Booth, R. S. 1994, A&A 281, 871-881
Palmer, P., Gardner, F. F., Whiteoak, J. B. 1984, MNRAS 211, 41P
Pavlakis, K. G., Kylafis, N. D. 1996, ApJ 467, 300
Pavlakis, K. G., Kylafis, N. D. 1996, ApJ 467, 309
Pavlakis, K. G., Kylafis, N. D. 2000, ApJ 534, 770
Radford, H. E. 1961, Phys. Rev. 122, 114
Reid, MJ̇., Haschick, A. D., Burke, B. F., Moran, J. M., Johnston, K. J., Swenson, G. W. 1980 ApJ 239, 89
Smits, D. P. 1994, MNRAS 269, L11
Smits, D. P. 1997, MNRAS 287, 253
Smits, D. P., Cohen, R. J., Hutawarakorn, B. 1998, MNRAS 296, L11
Sutton, E. C., Sobolev, A. J., Ellingsen, S. P., Cragg, D. M., Mehringer, D. M., Ostrovskii, A. B., Godfrey, P. D. 2001, ApJ 554, 173
Szymczak, M., Kus, A. J., Hrynek, G. 2000, MNRAS 312, 211
Zuckerman, B., Palmer, P. 1970, ApJ 159, L197

Mon. Not. R. Astron. Soc. **000**, 000–000 (0000) Printed 1 February 2008 (MN LATEX style file v2.2)

Erratum: A search for 4765-MHz OH masers in Southern Star Forming Regions

R. Dodson [1], M.A. Voronkov [2,3], S.P. Ellingsen [4]

[1] *ISAS, Yoshinodai 3-1-1 , Sagamihara, Kanagawa 229-8510, Japan*

[2] *Australia Telescope National Facility, CSIRO,Locked Bag 194, Narrabri, NSW 2390, Australia*

[3] *Astro Space Centre, Profsouznaya st. 84/32, 117997 Moscow, Russia;*

[4] *School of Mathematics and Physics, University of Tasmania, GPO Box 252-21, Hobart, Tasmania 7001, Australia*

1 February 2008

ABSTRACT

Dodson & Ellingsen (2002) included several observations with significant pointing errors, invalidating the upper limits found in these directions. These have now been reobserved or recalculated. A new table of upper limits has been generated, and two more masers that would have been seen have been found.

Key words: HII regions — ISM: molecules — masers — radio lines : ISM

1 OBSERVATIONS

Our followup to the original observations (Dodson & Ellingsen 2002), performed on 15 December 2003, with the ATCA in configuration 6A, had only 10 baselines so the detection limits are a little higher than the original data set and are listed in Table 1. As before the detection peak heights, velocities and widths are found from a Gaussian fit to the unsmoothed data. The detections are listed in Table 2.

G339.622-0.121

The 4765-MHz maser emission from this new detection peaks at -37.0 km s^{-1}. This site has 1720-, 1665- and 6035-MHz OH masers (Caswell 1999). There is a nearby 1612-MHz emission

Table 1. Sources searched for 4765-MHz OH maser emission. The 5-σ limit column is for emission in a vector averaged spectrum at centred on the position, and covering the velocity range listed. References : a = Caswell (1997) ; c = Caswell (1999) ; d = Cohen et al. (1995) ;

Source Name	Reference position Right Ascension (J2000)	Declination (J2000)	Velocity Range (km s^{-1})	5-σ Limit (Jy)	Central Velocity (km s^{-1})	References
		reobserved				
G339.622−0.121	16:46:06.030	-45:36:43.90	-130–95	0.11	-36.7	c
G347.628+0.149	17:11:50.888	-39:09:29.00	-130–95	0.12	-96.7	a
G348.550−0.979	17:19:20.418	-39:03:51.65	-130–95	0.12	-13.0,-12.1	a,c
G351.581−0.353	17:25:25.085	-36:12:46.08	-130–95	0.15	-93.8	a
		corrected				
G351.417+0.645	17:20:53.370	-35:47:01.16	-106–135	0.11	-10.0,-10.4	a,c
*IRAS*17175−3544	17:20:54.945	-35:47:02.38	-106–135	0.11	-10.0	d
G351.775−0.536	17:26:42.559	-36:09:15.99	-106–135	0.15	-8.7,4	a,c

Table 2. Sources with detected 4765-MHz OH emission. References : *=new source, e=Smits (2003);

Source Name	4765-MHz Maser Right Ascension (J2000)	Declination (J2000)	Peak Flux Density (Jy)	Velocity of Peak (km s^{-1})	Width of Peak (km s^{-1})	References
G339.622−0.121	16:46:06.03±0.04	-45:36:43.3±0.2	0.56	-37.0	0.5	*
G347.628+0.149	17:11:51.01±0.02	-39:09:29.0±0.5	3.65	-96.3	0.3	e

site which also displays methanol masing. In this region there is no detectable 4765-MHz emission. The flux from this source is below the limit of Smits (2003).

G347.628+0.148

This source was discovered by Smits (2003), with a slightly stronger flux density (a peak of 5 Jy). As the source is very narrow (0.3 km/s FWHM) our observations may underestimate the strength, but the measured emission was falling during the Hartsebethock observations and is consistent. This source has a peak velocity of -96.3 km s^{-1} and a secondary peak of 0.3 Jy at -95.1 km s^{-1} from the same position. This source also has emission from 1612-, 1665-, 1720- and 6035-MHz, and 6.7-GHz methanol. It is an UCHII region.

2 CONCLUSIONS

Both sources found also display 1720- and 6035-MHz OH emission, so they do not significantly alter our previous conclusions about the association of 4765-MHz OH emission with these two transitions.

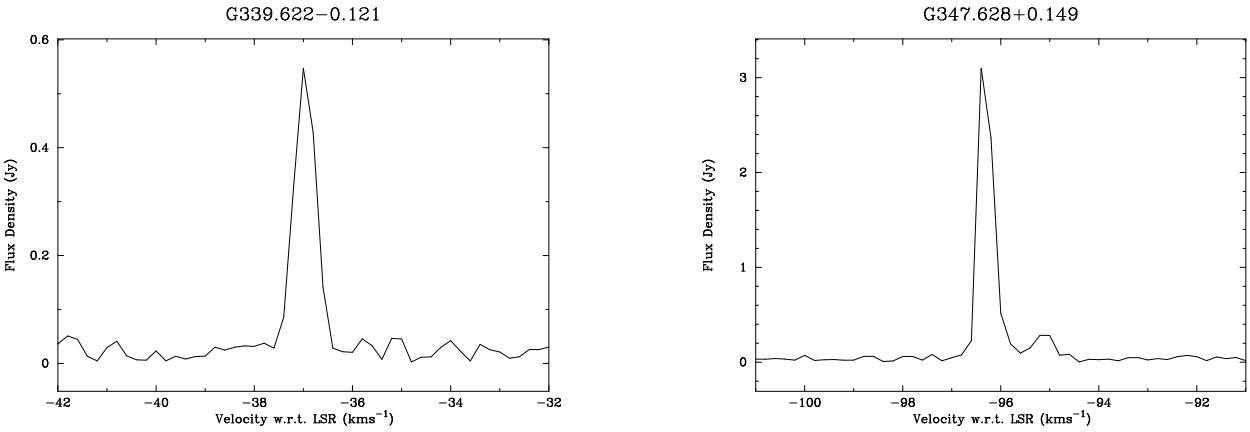

Figure 1. Total intensity spectra of the 4765 MHz OH masers reobserved with the ATCA

3 ACKNOWLEDGMENTS

We would like to thank Derck Smits for drawing our attention to the error in the original paper.

REFERENCES

Caswell, J. L. 1997, MNRAS 289, 203

Caswell, J. L. 1999, MNRAS 308, 683

Cohen, R. J., Masheder, M. R. W., Caswell, J. L. 1995, MNRAS 274, 808

Dodson R. G., Ellingsen S. P., 2002, MNRAS, 333, 307

Smits D. P., 2003, MNRAS, 339, 1